Experimental Verification of Darcy-Brinkman-Forchheimer Flow Model for Natural Convection in Porous Media

N. Kladias* and V. Prasad†
Columbia University, New York, New York 10027

Experimental results for natural convection in a horizontal porous cavity of aspect ratio, $A = 5$, and heated from below are reported. A wide range of governing parameters are covered by careful selection of beads size, solid material, and fluid. These results fully support the effects of fluid flow parameters (Rayleigh and Prandtl numbers), porous matrix structure parameters (Darcy and Forchheimer numbers), and the conductivity ratio as predicted by the formulation based on the Darcy-Brinkman-Forchheimer (DBF) equations of motion. The DBF flow model, with variable porosity and variable thermal conductivity in the wall regions, predicts reasonably well in comparison with the experimental data. However, the difference between the predictions and the measurements increases as the ratio of solid-to-fluid thermal conductivity becomes very large.

Nomenclature

A = aspect ratio, W/H
b = porous matrix structure property associated with inertia term, m
c = isobaric specific heat, J/kg · K
Da = Darcy number, Eq. (8)
Fs = Forchheimer number, Eq. (9)
g = acceleration due to gravity, m/s^2
H = height of saturated porous layer, m
k = thermal conductivity, W/m · K
k_m = stagnant thermal conductivity of porous medium, W/m · K
K = permeability of porous matrix, m^2
m = wave number
Nu = overall Nusselt number, Eq. (4)
Nu_f = overall Nusselt number based on fluid conductivity, Eq. (5)
Pr^* = modified Prandtl number, λPr_f
Pr_f = fluid Prandtl number, Eq. (7)
Ra^* = Darcy-modified Rayleigh number, $\lambda Ra_f Da$
Ra_f = fluid Rayleigh number, Eq. (6)
t = time, s
T = temperature, K
V = filtration velocity vector, m/s
W = width of porous layer, m
α = thermal diffusivity of fluid, $k/\rho c$, m^2/s
α_m = thermal diffusivity of porous medium, $k_m/(\rho c)_f$, m^2/s
β = isobaric coefficient of thermal expansion of fluid, 1/K
ε = porosity
γ = dimensionless particle diameter, d/H
λ = conductivity ratio, Eq. (10)
Λ = viscosity ratio, Eq. (11)
μ = dynamic viscosity of fluid, kg/m · s
μ' = apparent dynamic viscosity for Brinkman's term, kg/m · s
ν = kinematic viscosity of fluid, m^2/s
ρ = density, kg/m^3

Subscripts
c = critical value for the onset of convection
f = fluid
m = fluid-saturated porous medium, also, mean value
s = solid
∞ = value in bulk medium

Received April 16, 1990; revision received Oct. 29, 1990; accepted for publication Oct. 30, 1990.

*Currently, Webster Research Center, Xerox Corporation, North Tarrytown, NY 10591.
†Department of Mechanical Engineering. Member AIAA.

Introduction

NATURAL convection in horizontal porous layers heated from below is one of the classical heat transfer problems that have been investigated extensively. Several theoretical studies that predict the conditions for the onsets of stable and oscillatory convection regimes and the heat transfer rates have been reported in the literature.[1-3] Experimental studies dealing with the horizontal porous layer problem are, however, limited. In addition to the early works of Wooding, Schneider, Elder, Katto and Masuoka, and Kaneko et al., the heat transfer experiments were also conducted by Combarnous and coworkers, Yen, Buretta and Berman, Bau and Torrance, and Jonsson and Catton (see the review articles by Combarnous and Bories,[1] Cheng[2] and Catton[3]).

Schneider's data for various porous media showed a large scale variation in heat transfer rate as a function of the fluid-solid combination and the grain size.[4] Similar divergence was also observed by Combarnous,[5] Buretta and Berman,[6] and others. Combarnous's data revealed that when the Darcy-modified Rayleigh number Ra^* is about 240–280, the convective motion changes in character, which is indicated by a change in the slope for Nusselt number curve. This new regime of fluctuating convection was addressed later by Caltagirone,[7] Schubert and Straus,[8] Kimura et al.[9] and others. A compilation of experimental data and theoretical results (based on the Darcy flow model) by Cheng[2] shows that the predictions agree with the experimental data only for the water-glass media at low Ra^*.

Various theories have been proposed to explain this divergence in the experimental data. Considering the argument that, by increasing convection, the influence of the thermal conductivity of porous layer decreases and moves closer to the fluid conductivity, Schneider[4] modified his results and presented them based upon the fluid conductivity. This resulted in a closer agreement between the Nusselt numbers for various porous media at high Rayleigh numbers, but introduced divergence at low Ra^*.

Combarnous and Bories[1] attributed the cause of the divergence to the nonvalidity of the assumption of an infinite heat transfer coefficient between the fluid and solid particles, and proposed a two-phase model. The use of this model introduces

two more variables besides Ra^* that are very difficult to estimate. Although the model is more realistic, the use of it is cumbersome and the results depend on the right choice for several unknown quantities. The numerical results obtained by using this model could not show any better agreement with the experimental data. Some other investigators[10–12] argued in favor of considering the modified Prandtl number Pr^*, in addition to Ra^*, to explain the divergence in the heat transfer data.

Prasad et al.[13] suggested that the major cause of divergence in the Nu-Ra^* relation is not an explicit effect of Prandtl number but the use of an improper thermal conductivity for the porous medium. Utilizing on the fact that the fraction of energy transported by the fluid increases with the Rayleigh number, they presented a model for an effective thermal conductivity that takes into account the enhanced effect of fluid thermal conductivity as a function of the convective flow. They concluded that there exists a unique relationship between the Nusselt and modified Rayleigh numbers, unless the conditions assuring the validity of Darcy's law are violated, and showed that the ratio of the layer width over the particle size γ is a parameter of interest for the breakdown of Darcy's law.

An attempt to correlate the diverse measurements of heat transfer in fluid-saturated porous media heated from below has been also made by Wang and Bejan.[14] These authors considered only the Darcy and Forchheimer asymptotes of the phenomenon and, based on the scale analysis arguments, they suggested that, in the Forchheimer flow regime, the Nusselt number must increase as $(Ra\ Fs/Pr^*)^{1/2}$. They found that this correlation has a better agreement with the experimental data than the Darcy solutions of other authors. However, it does not provide a complete description of the heat transfer behavior, since under certain conditions the viscous drag and wall channeling effects may be quite significant and have not been accounted for in this correlation.

In recent years, extensive research efforts have been devoted to developing a mathematical model that can predict accurately convective flows and heat transfer in porous media. Generally, the Darcy-Forchheimer, the Darcy-Brinkman, or the Darcy-Brinkman-Forchheimer (DBF) equation of motion has been employed, together with continuity and (one) energy equations. The importance of the porosity variation in the wall region and the dispersion effects have also been investigated. Theoretical studies employing these models can be found in contemporary literature, and cover both external and internal flows. Here, we will restrict our discussion to the horizontal porous layers only.

Rudraiah[15] was probably the first to consider the Darcy-Brinkman model to study Benard convection in porous media, and to recognize the importance of Darcy number other than Ra^* in producing the instability. Kvernvold and Tyvand[16] employed a second-order dispersion model to demonstrate the effect of Da. Georgiadis and Catton[17] obtained solutions for the DBF model, and noted that the divergence in heat transfer results is primarily due to inertia effects. Later, they emphasized the importance of the dispersion models.[18] We have also conducted a series of theoretical studies employing the DBF model,[19–22] and have examined, for the first time, the effect of variable porosity in a horizontal porous layer problem.[21,22] Since our previous theoretical studies form a basis for the present experimental work, they will be reviewed separately.

From the review of the literature on natural convection in porous media, it is evident that no extensive experimental study on a large variety of solid-fluid combinations, which would isolate and fully characterize the contribution of the solid matrix structure and the effect of the fluid properties, has been reported thus far. The only exceptions are the works of Georgiadis and Catton[17] and David et al.,[23] which attempted to compare with the experimental data of Jonsson and Catton[10] and Combarnous[5] for a horizontal layer, and of Prasad et al.[13] for a vertical annulus, respectively. Indeed, a large body of literature has been reported on non-Darcy convection in porous media, without any proper experimental verification of the suitability of the model being used.

The purpose of the present study is, thus, to conduct experiments for a wide range of governing parameters, and to verify the validity of the mathematical formulation based on the DBF equations of motion. The primary objectives of the experiments are as follows:

1) To study the effects of Darcy and Forchheimer numbers by changing the size of the solid particles (i.e., bead diameter) for a given aspect ratio A and Prandtl number Pr_f

2) To examine the effects of Prandtl number Pr_f by changing the saturating fluid for fixed values of Da, Fs, and A

3) To characterize the effect of the conductivity ratio λ by changing the solid-fluid combinations for given Da, Fs, and A

4) To establish Nusselt-vs-Rayleigh number relationships for various values of Da, Fs, Pr_f, and λ

5) To verify the suitability of the DBF model with variable porosity and variable thermal conductivity in the wall region by comparing the experimental data with the theoretical results

Experimental Apparatus and Procedure

To model a horizontal cavity heated from below at a constant temperature and isothermally cooled at the top, an experimental apparatus (Fig. 1) was designed and fabricated in the following way. First, a base plate of 381 × 381 mm^2 and 10 mm thick was made out of brass. In order to vary the heat input as a function of location, ten thermofoil heaters were cemented at the back of this brass plate, which was then placed in a recess made in a 25.4 mm thick plexiglass plate. High temperature grease was used to eliminate any air gap between the brass plate and the plexiglass surface. Five thermofoil heaters were then cemented at the back of the plexiglass bottom plate to guard against the conduction heat losses. Another 25.4 mm thick plexiglass plate was then used as the base for this bottom plate, further reducing the heat losses. The heater leads were taken out through the slots made in the bottom wall and at the base of the cavity. Fluke 8050A digital multimeters were used to record the voltage and current in each heater circuit, with an accuracy of 0.5 and 1%, respectively.

The top wall was made out of 6 mm thick aluminum plate attached to the bottom side of a plexiglass plate with slots in it for cooling water circulation. Two constant temperature circulators, with 0.1°C control accuracy, were used to supply water at about room temperature. The cold plate could be positioned at different heights with the help of four bar screws. The side walls of the cavity were made of 25.4 mm thick plexiglass, 400 mm high.

Forty thermocouples, made out of 30 AWG teflon coated copper-constantan wires, were attached to the brass plate. Sixteen of these thermocouples were placed in a line midway of the bottom surface. The rest were placed at other locations to check the uniformity of temperature at the bottom surface. The wires were run through the slots already made in the brass plate, and were taken to one end of the plate. The slots were then filled with plastic-steel epoxy cement and sanded to have a smooth surface. A similar arrangement was used for recording the top plate temperature at twenty-four locations. Twelve thermocouples cemented on the top surface of the bottom wall and another twelve cemented in symmetric positions on the lower side of the bottom wall were used to record the temperature distributions. This information was used to calculate the heat losses through the bottom of the cavity. The thermocouples were connected to a Fluke 2400B digital data acquisition system with programmable control output signals and automatic fixed-time interval scanning. The readings were displayed and stored in an IBM personal com-

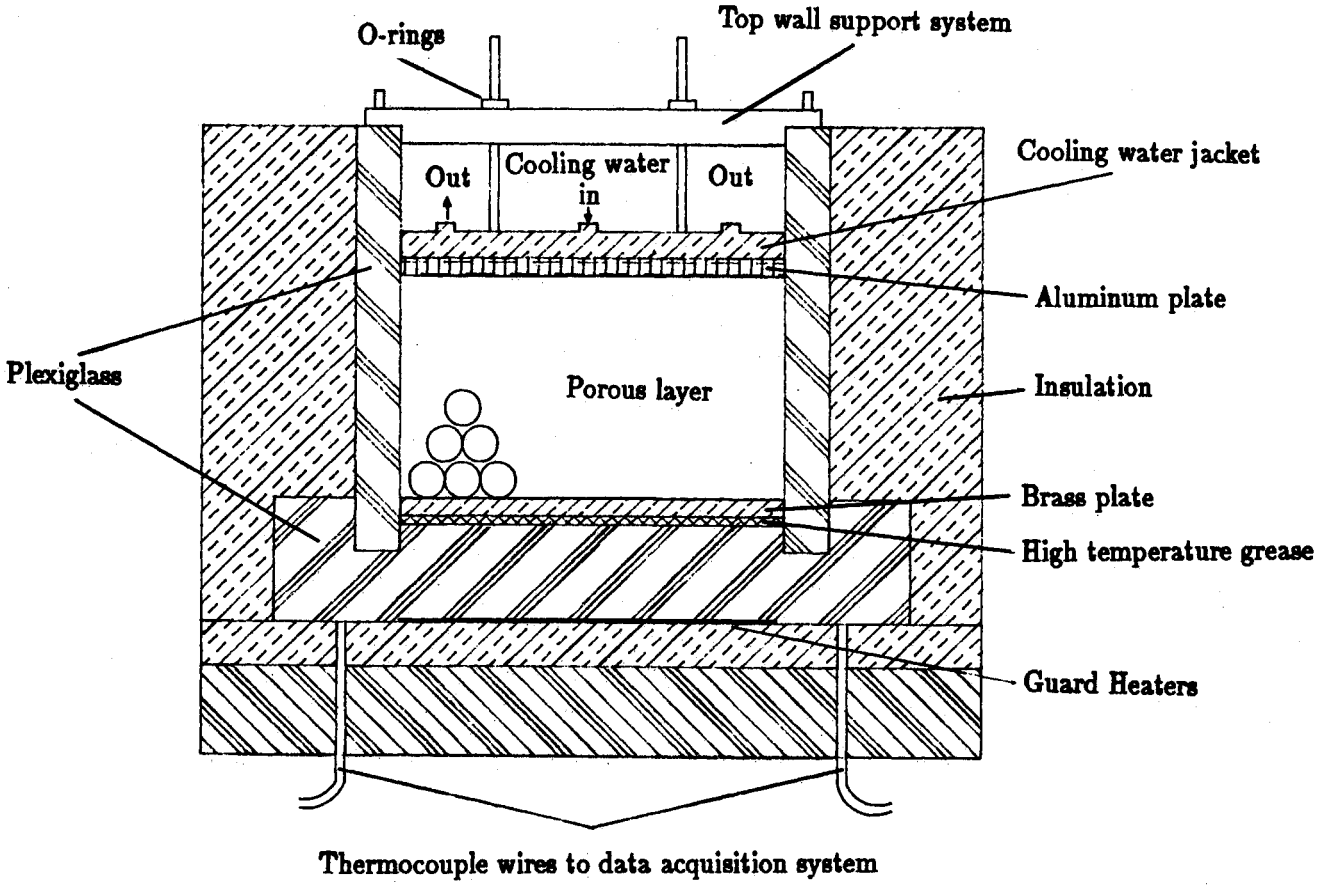

Fig. 1 Schematic of experimental apparatus.

Table 1 Solid-fluid combinations and range of Darcy and Forchheimer numbers for the present experimental data

Set no.	Fluid	Solid	d, mm	ε	$Da \times 10^5$	$Fs \times 10^3$	Ra^*	$Ra_f \times 10^{-6}$	Pr_f	λ
1	Water	Glass	3	0.375	0.116	0.74	27–625	37.5–732	5.48	0.73
2	Water	Glass	6	0.396	0.583	1.52	85–2104	19.6–486	5.40	0.74
3	Water	Glass	15	0.453	7.780	4.31	624–15,658	10.1–255	5.06	0.79
4	Water	Glass	25	0.468	18.50	6.99	700–27,172	4.8–185	5.06	0.79
5	Water	Acrylic	12.7	0.395	2.580	3.21	395–13,029	8.7–288	5.71	1.75
6	Water	Acrylic	25.4	0.461	20.80	7.22	4115–91,303	12.2–272	6.21	1.61
7	Water	Steel	6.35	0.388	0.604	1.59	4–289	5.3–359	5.64	0.13
8	Water	Steel	15.87	0.444	6.850	4.37	34–1552	2.9–133	5.88	0.17
9	Glycol	Glass	3	0.400	0.153	0.77	10–93	14.6–137	112.8	0.44
10	Glycol	Glass	6	0.440	0.934	1.64	20–647	4.5–134	125.2	0.48
11	Glycol	Glass	25	0.463	18.40	6.99	1385–6429	15.2–71	132.4	0.49
12	Glycol	Acrylic	25.4	0.463	21.20	7.23	1471–30,091	5.7–116	131.4	1.22
13	Glycol	Steel	15.87	0.454	8.37	4.53	66–1288	5.54–103	141.4	0.14
14	Heptane	Glass	25	0.468	18.50	6.99	16,057–226,320	240–3390	6.11	0.36
15	Heptane	Acrylic	25.4	0.456	19.70	7.14	75,803–652,436	416–3580	6.00	0.93
16	Heptane	Steel	15.87	0.444	6.840	4.37	7891–28,217	1033–3658	5.70	0.11

puter. Using this system, we could read temperatures up to the first decimal place with an accuracy of 0.2°C.

For our heat transfer calculations, we have used the temperature measurements of the twenty-eight thermocouples (sixteen at the bottom and twelve at the top) placed on a line midway from the sides, as previously described. The dimensions of our cavity reduced to a large extent the effect of side walls on the measurements in the vertical middle plane. In this respect, our choice of cavity dimensions was similar to that of Combarnous[5] (37 × 61 cm^2, A = 6.9), Combarnous and Bories[1] (46.3 × 66.3 cm^2, A = 11.9), Buretta and Berman[6] (30.5 cm diam, $3.5 \leq A \leq 7$), and Jonsson and Catton[10] (17.5 cm diam, $1.2 \leq A \leq 7$).

A large number of solid-fluid combinations was used in the present experiment. The size and material of the solid beads, as well as of the saturating fluids, were carefully selected in order to achieve large variations in the parameters of interest. A complete overview of the solid materials, the grain sizes, and the saturating fluids is presented in Table 1. The thermophysical properties of the solid and fluid components were obtained at the mean temperatures $(T_h + T_c)/2$. In our experiments, the ratio of cavity height-to-bead diameter varied between 3 and 25.4. Low values of height-to-bead diameter ratio were necessary in order to analyze the non-Darcy effects in detail.

The porosity of the porous matrix was calculated from the weight of the solid beads used to fill the cavity and its measured density. The permeability K and the inertial resistance coefficient b were calculated by employing the Ergun model:

$$K = [\varepsilon^3/150(1 - \varepsilon)^2]d^2 \quad (1)$$

$$b = [1.75/150(1 - \varepsilon)]d \quad (2)$$

The stagnant thermal conductivity of the working medium was obtained from the correlations of Kunii and Smith, which predict k_m reasonably well.[24] In some cases, it was possible to measure k_m with the present arrangement by achieving $Ra^* < 4\pi^2$ (pure conduction) for very low Da (see Prasad et al.[24]).

Temperatures on the bottom and top surfaces of the cavity were checked at regular intervals to make sure they were maintained at isothermal conditions. Power in the heaters was changed according to the temperature distribution on the bottom surface. Achieving a constant temperature boundary condition was a difficult task, especially in the present case, where the heat transfer rate is a highly nonlinear function of the spatial coordinates. However, we managed to keep the maximum variation on any surface within 5% of the average temperature of that surface by performing between four and ten adjustments of the power input to the heaters.[22] The number of power adjustments was dependent on the solid-fluid combinations and the initial power distribution. To make sure that the steady-state conditions had been achieved, sufficient time (4–10 h after the last power adjustment) was allowed before the measurements were taken. More time (24–36 h) was required for steady-state conditions at low values of Ra^*, due to the relatively strong diffusive heat transfer. The fluctuations of temperature at the bottom and top surfaces at very high values of Ra^* were minimal.

To eliminate the conduction losses through the side walls of the cavity, 80 mm thick fiberglass insulation was wrapped tightly around the side walls of the cavity; also, additional insulation was used at the bottom of the cavity (Fig. 1). The conduction losses through the bottom of the cavity were generally within 5–10% of the power input. The conduction loss from the side walls was estimated to be negligible. Several sets of measurements were taken by changing the bottom surface temperature T_h for each solid-fluid combination to establish its own trend. Further details on the experimental arrangement and procedure and the estimation of losses may be found in the doctoral dissertation of N. Kladias.[22]

The uncertainty in the thermophysical properties was estimated at approximately 2%, on the basis of differences in values found in the literature. The error in the temperature measurement was estimated as 1.5%. The uncertainty in the measurement of the power input was 1%, as was the error in the measurement of dimensions. Based upon these fractions, the uncertainties due to measured quantities and thermophysical properties for the Rayleigh number and Nusselt number are about 5.5% and 6%, respectively. In calculating these uncertainties, the inhomogeneity and anisotropy of the porous medium, and the inaccuracy of the empirical relation used for calculating the matrix structure properties, have not been considered.

The heat transfer coefficient on the bottom wall was calculated as

$$h = [\text{net power input}]/[\text{bottom surface area} \times (T_h - T_c)] \quad (3)$$

The Nusselt number Nu was then obtained by using the stagnant thermal conductivity k_m and the height of the layer H, as

$$Nu = hH/k_m = \lambda Nu_f \quad (4a)$$

where the mean Nusselt number based on the fluid thermal conductivity is given by

$$Nu_f = hH/k_f \quad (4b)$$

Qualitative Observations from DBF Solutions

Here we shall briefly discuss the conclusions of our previous publications,[19–22] which presented numerical results based on the DBF model. This will make clearer the qualitative agreement between the DBF solutions and the measurements. The governing equations for isotropic and homogeneous porous media (without porosity and thermal conductivity variations) are written as[19–23]

$$\nabla \cdot V = 0 \quad (5a)$$

$$\frac{\rho_f}{\varepsilon}\frac{\partial V}{\partial t} + \frac{\rho_f}{\varepsilon^2}(V \cdot \nabla)V = -\nabla p + \rho_f g - \frac{b}{K}|V|V - \frac{\mu}{K}V + \mu'\nabla^2 V \quad (5b)$$

$$(\rho c)_m \frac{\partial T}{\partial t} + (\rho c)_f (V \cdot \nabla)T = k_m \nabla^2 T \quad (5c)$$

A dimensional analysis of these equations shows that the steady-state free convection in saturated porous media is governed by the following parameters:

$$\text{fluid Rayleigh number, } Ra_f = g\beta H^3(T_h - T_c)/\nu\alpha_f \quad (6)$$

$$\text{fluid Prandtl number, } Pr_f = \nu/\alpha_f \quad (7)$$

$$\text{Darcy number, } Da = K/H^2 \quad (8)$$

$$\text{Forchheimer number, } Fs = b/H \quad (9)$$

$$\text{conductivity ratio, } \lambda = k_f/k_m \quad (10)$$

$$\text{viscosity ratio, } \Lambda = \mu'/\mu \quad (11)$$

and porosity ε. Three of these parameters—porosity, ε, Darcy number, Da, and Forchheimer number, Fs—are the porous matrix structure parameters, whereas the Rayleigh and Prandtl numbers, Ra_f and Pr_f, depend on only the fluid properties. The conductivity ratio λ and viscosity ratio Λ, on the other hand, depend on both the solid and fluid properties.

The numerical solutions for uniform porosity media show that the convective flow is initiated at lower fluid Rayleigh number Ra_f than that predicted by the linear stability analysis for the Darcy flow model. The effect is considerable, particularly at $Da > 10^{-4}$. On the other hand, an increase in the thermal conductivity of solid particles has a stabilizing effect. Also, the Rayleigh number Ra_f, required for the onset of convection increases as the fluid Prandtl number is decreased. In the stable convection regime, the heat transfer rate increases with the Rayleigh number, the Prandtl number, the Darcy number, and the ratio of solid-to-fluid thermal conductivity. However, there exists an asymptotic convection regime where the porous media solutions are independent of the permeability of the porous matrix or Darcy number. In this regime, the temperature and flow fields are very similar to those obtained for a fluid layer heated from below. Indeed, the Nusselt numbers for a porous medium with $k_f = k_s$ match with the fluid results. The effect of Prandtl number is observed to be significant for $Pr_f < 10$, and is strengthened with an increase in Ra_f, Da, and k_s/k_f.[19–22] On the other hand, the effects of porosity and specific heat ratio are not significant in the stable convection regime.[21,22]

The solutions for variable porosity media show that the convective heat transfer is greatly enhanced when the wall channeling, due to variation in porosity, is considered. Also, the nonhomogeneous porous media solutions approach the fluid solutions for $Da \geq 10^{-4}$, which is much lower than the corresponding Darcy number ($Da \geq 10^{-2}$) in the case of a homogeneous porous layer.[21,22] Many of these observations are supported also by the works of Beckerman et al.,[25] Lauriat and Prasad,[26] and David et al.[27] on vertical enclosures.

Experimental Results and Discussion

Experimental results for horizontal porous layers of $A = 5$ were obtained for wide ranges of governing parameters (Table 1). Figure 2a presents the experimental data in the usual $ln(Nu)$-vs-$ln(Ra^*)$ plot. As expected, a divergence in the overall Nusselt number Nu is observed, which depends on the solid-fluid combinations of the convective medium. The divergence in the present heat transfer results is very similar to that reported by previous investigators.[2,13] However, the previous experimental studies on horizontal porous layers have been limited to low values of modified Rayleigh number, $Ra^* \leq 10^3$, whereas, in the present study, Ra^* on the order of 10^6 has been achieved (see Table 1 and Fig. 2a). Moreover, we were able to achieve Darcy numbers on the order of 10^{-4}, whereas the reported values of Darcy number are $Da \leq 10^{-5}$. Figure 2b, on the other hand, presents the heat transfer results in terms of fluid Rayleigh and Nusselt numbers. These figures clearly show that the magnitude of the divergence in measured heat transfer rates depends on Rayleigh number, particle size, Prandtl number, and conductivity ratio. The various theories proposed to explain this divergence have been discussed earlier. In this section, first, a comparison between our measurement and the published experimental results is presented. Then, the divergence is explained in terms of the porous matrix scaling parameters and the thermophysical properties of the constituents of porous media. Finally, the experimental results are compared with the numerical predictions, based on the DBF model.

Comparison with Reported Experimental Data

A comparison of our experimental results with the data of Schneider,[4] Combarnous,[5] Buretta and Berman,[6] Jonsson and Catton,[10] and Yen[28] is presented in Fig. 3. The comparison is limited to low values of Ra^* since, as was mentioned earlier, the highest reported values of Ra^* for horizontal porous layers are of the order of 10^3. Excellent agreement is obtained for a steel-water medium (d = 6.85 mm) and glass-water media (d = 3 and 6 mm). For example, our Nusselt numbers for a 6.85 mm steel-water porous system agree with the results reported by Jonsson and Catton[10] for a 4.84 mm steel-water medium within 4.9% at $Ra^* = 110$ and 2.9% at $Ra^* = 170$, and our results for a 6 mm glass-water medium are in agreement with their results within 5.6% at $Ra^* \approx 250$ and 6.1% at $Ra^* = 800$. We found best agreement with the experimental data of Yen,[28] since the layer depth of his experimental runs was identical to the present value, $H = 76.2$ mm. Our data for a 6 mm glass-water medium are within 2% of the results for the same medium reported by Yen. On the other hand, Buretta and Berman's[6] results for a 6 mm glass-water medium are closer to our 3 mm glass-water results than to our 6 mm glass-water results. The main reason for this is probably the different geometric configuration used in their experiments (a cylindrical cavity). Therefore, no further attempt was made to compare our results with theirs for larger glass beads. Also, the largest bead diameter used by the other investigators was 10 mm[5] and, therefore, no comparison is possible with our 15 mm and 25 mm glass beads experiments. Additionally, no comparison can be made for many solid-fluid combinations used in our experiments, other than the glass-water and steel-water, since there are no previous experiments with those combinations.

Another encouraging fact for the accuracy of our experimental results is that for solid-fluid combinations, where small modified Rayleigh numbers could be achieved, i.e., 3 mm glass-water, 6.35 mm steel-water, 3 mm glass-glycol, and 6 mm glass-glycol, we obtained the onset of convection ($Nu \approx 1$) at $Ra^* \approx 40$ (Fig. 2a), a value which has been established analytically and experimentally.[1-3] Moreover, our experimental data for 3 mm glass-water porous layer at low Ra^* are in very good agreement with the predicted Nusselt number from the correlation, $Nu = Ra^*/40^2$.

Heat Transfer Results and Discussion

Here, we shall attempt to show the qualitative agreement between the predictions and the experimental results. The numerical solutions were obtained using Eqs. (5a–c). A sinusoidal temperature distribution was used to initiate the finite-difference calculations. The details of the mathematical model and the alternate direction implicit numerical scheme are omitted here for brevity and can be found elsewhere.[19-22]

Effect of Darcy and Forchheimer Numbers

Darcy and Forchheimer numbers vary with the particle size d and the porosity ε, as given by Eqs. (1), (2), (8), and (9), which yields

$$Fs = C(\varepsilon)Da^{05} \tag{12}$$

Therefore, the effect of these parameters can be studied experimentally, if we consider the results for porous systems with the same solid-fluid combination but different particle sizes. In this case, the Prandtl number and the conductivity ratio are kept constant. The results can be presented in terms of Darcy number since, for a particular porous medium, Forchheimer number is correlated to Da, according to Eq. (14).

First, consider the heat transfer results for glass-water media, as presented in Fig. 2a in terms of the average Nusselt number Nu as a function of the modified Rayleigh number Ra^* and the Darcy number Da. It is clearly seen that the Nusselt number is higher for the lower Darcy number (densely packed) porous system (3 mm beads). At higher Darcy numbers (larger particle size), a branching occurs and Nu decreases as Da increases. Indeed, for $Ra^* = 700$, the Nusselt number for a 25 mm glass-water medium is 34.5% lower than the Nusselt number for a 6 mm glass-water medium. The trend of decreasing Nusselt number with increasing particle size (or Darcy number), for constant Ra^* has been reported in the literature many times. However, as was made clear in our earlier publications,[19-22] the presentation of results in terms of the fluid Rayleigh number Ra_f, rather than in terms of the modified Rayleigh number Ra^*, reveals the true effects of Darcy number. Indeed, our data for glass-water porous systems, presented in terms of Ra_f and Nu_f (Fig. 4a), clearly show the trend of increasing heat transfer with Da, or the permeability of the porous matrix. It is also observed that the heat transfer curves for densely packed media, i.e., 3 mm beads ($Da = 1.16 \times 10^{-6}$) and 6 mm beads ($Da = 5.84 \times 10^{-6}$), are almost parallel. However, the slope of the curve changes substantially with an increase in Da. This is clearly seen from the 15 mm glass-water ($Da = 7.78 \times 10^{-5}$) and the 25 mm glass-water ($Da = 1.85 \times 10^{-4}$) data. It is interesting to note that the experimental results confirm our theoretical prediction that the Nusselt number curves for highly permeable porous systems ($Da > 10^{-4}$), with $k_s \approx k_f$, approach the Nusselt number curve for a fluid-filled cavity at high Ra_f. Indeed, at low Rayleigh numbers, the 25 mm glass-water Nusselt numbers are much lower than the pure water Nusselt numbers (Fig. 4a), but the difference decreases as Ra_f increases. For example, the difference at $Ra_f = 10^7$ is 51.5%, which decreases to 29% at $Ra_f = 1.25 \times 10^8$.

The above trend becomes more distinct in Fig. 4b, which is a compilation of our experimental results for 25 mm glass-water, pure water, 25 mm glass-heptane, and pure heptane. By using heptane, whose Prandtl number is close to water, we were able to eliminate the Prandtl number effect and, thus, extend our glass-water and pure water results to higher values of Ra_f. However, due to the small difference in the conductivity ratio between glass-heptane ($\lambda \approx 0.36$) and glass-water ($\lambda \approx 0.79$) media, the glass-heptane heat transfer results are slightly higher than the glass-water results. It can now be clearly seen that the 25 mm glass-heptane Nusselt numbers approach those for pure heptane. For $Ra_f > 10^9$, the heat transfer rates are seen to be almost identical. This agrees with

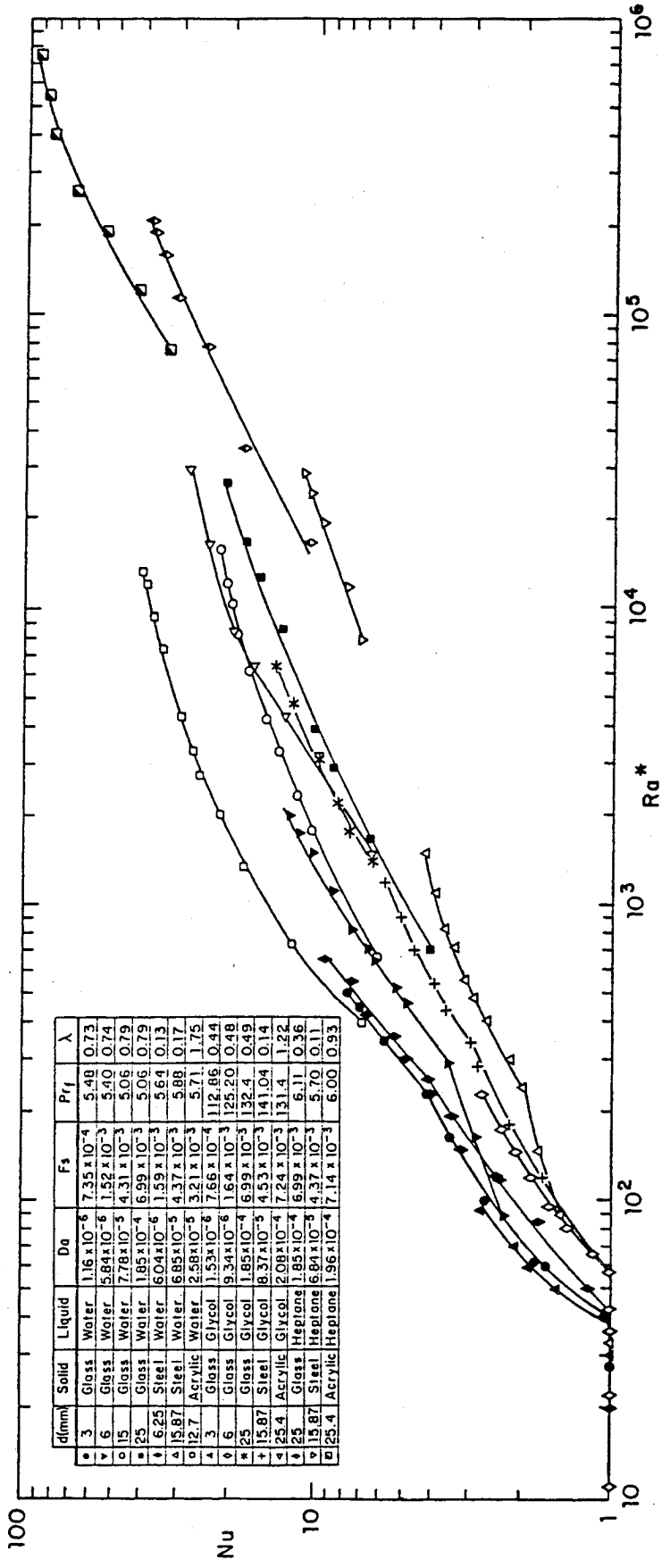

d(mm)	Solid	Liquid	Da	Fs	Pr_f	λ
● 3	Glass	Water	1.16×10^{-6}	7.35×10^{-4}	5.49	0.73
▼ 6	Glass	Water	5.84×10^{-6}	1.52×10^{-3}	5.49	0.74
○ 15	Glass	Water	7.78×10^{-5}	4.31×10^{-3}	5.06	0.79
■ 25	Glass	Water	1.85×10^{-4}	6.99×10^{-3}	5.06	0.79
♦ 6.25	Steel	Water	6.04×10^{-6}	1.59×10^{-3}	5.64	0.13
△ 15.87	Steel	Water	6.85×10^{-5}	4.37×10^{-3}	5.88	0.17
□ 12.7	Acrylic	Water	2.58×10^{-5}	3.21×10^{-3}	5.71	1.75
◁ 3	Glass	Glycol	1.53×10^{-6}	7.66×10^{-4}	112.86	0.44
◇ 6	Glass	Glycol	9.34×10^{-6}	1.64×10^{-3}	125.20	0.48
✱ 25	Glass	Glycol	1.85×10^{-4}	6.99×10^{-3}	132.4	0.49
+ 15.87	Steel	Glycol	8.37×10^{-5}	4.53×10^{-3}	141.04	0.14
◁ 25.4	Acrylic	Glycol	2.08×10^{-4}	7.24×10^{-3}	131.4	1.22
◆ 25	Glass	Heptane	1.85×10^{-4}	6.99×10^{-3}	6.11	0.36
▽ 15.87	Steel	Heptane	6.04×10^{-5}	4.37×10^{-3}	5.70	0.11
⊡ 25.4	Acrylic	Heptane	1.96×10^{-4}	7.14×10^{-3}	6.00	0.93

Fig. 2a Compilation of measured heat transfer rates for various solid-fluid combinations: Nusselt number based on k_m as a function of Darcy- modified Rayleigh number.

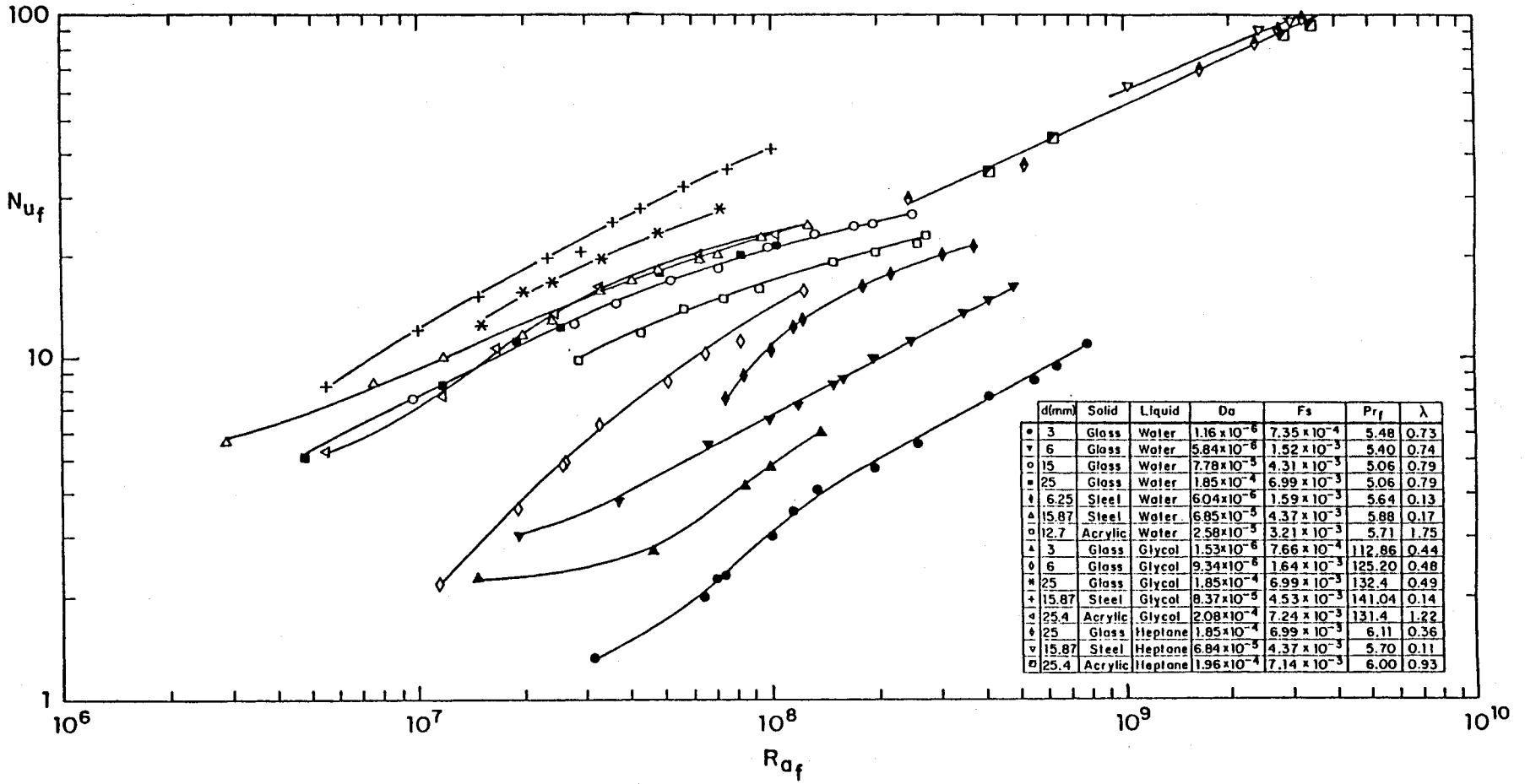

	d(mm)	Solid	Liquid	Da	Fs	Pr_f	λ
•	3	Glass	Water	1.16×10^{-6}	7.35×10^{-4}	5.48	0.73
▼	6	Glass	Water	5.84×10^{-6}	1.52×10^{-3}	5.40	0.74
o	15	Glass	Water	7.78×10^{-5}	4.31×10^{-3}	5.06	0.79
■	25	Glass	Water	1.85×10^{-4}	6.99×10^{-3}	5.06	0.79
♦	6.25	Steel	Water	6.04×10^{-6}	1.59×10^{-3}	5.64	0.13
△	15.87	Steel	Water	6.85×10^{-5}	4.37×10^{-3}	5.88	0.17
□	12.7	Acrylic	Water	2.58×10^{-5}	3.21×10^{-3}	5.71	1.75
▲	3	Glass	Glycol	1.53×10^{-6}	7.66×10^{-4}	112.86	0.44
◊	6	Glass	Glycol	9.34×10^{-6}	1.64×10^{-3}	125.20	0.48
*	25	Glass	Glycol	1.85×10^{-4}	6.99×10^{-3}	132.4	0.49
+	15.87	Steel	Glycol	8.37×10^{-5}	4.53×10^{-3}	141.04	0.14
◁	25.4	Acrylic	Glycol	2.08×10^{-4}	7.24×10^{-3}	131.4	1.22
◊	25	Glass	Heptane	1.85×10^{-4}	6.99×10^{-3}	6.11	0.36
▽	15.87	Steel	Heptane	6.84×10^{-5}	4.37×10^{-3}	5.70	0.11
⊡	25.4	Acrylic	Heptane	1.96×10^{-4}	7.14×10^{-3}	6.00	0.93

Fig. 2b Compilation of measured heat transfer rates for various solid-fluid combinations: Nusselt and Rayleigh numbers based on the fluid thermal conductivity.

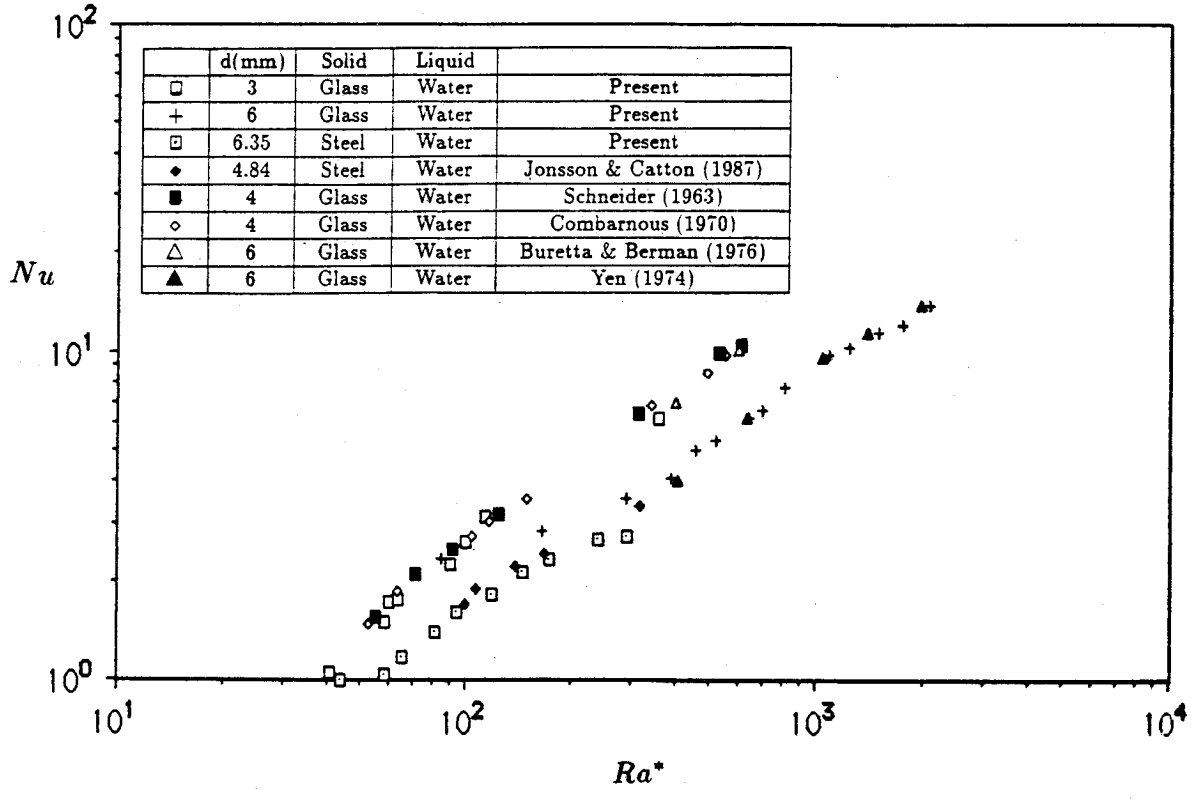

Fig. 3 Comparison with the published experimental data.

our theoretical predictions, and confirms the proposition that a properly formulated porous media mathematical model should yield the fluid results at high values of Darcy and Rayleigh numbers. This trend was also observed experimentally by Prasad et al. in the case of a vertical annulus.[13]

Conversely, the 6.35 mm steel-water and 15.87 mm steel-water results (Fig. 5) show the effect of Darcy number on the critical value of Rayleigh number for the onset of convection, $Ra_{f,c}$. It is easy to see that the onset of convection for the 15.87 mm steel-water porous system ($Da = 6.85 \times 10^{-5}$) is at $Ra_{f,c} = 1.6 \times 10^7$, whereas that for the 6.35 mm steel-water system ($Da = 6.04 \times 10^{-6}$) is at $Ra_{f,c} = 8 \times 10^7$. This agrees also with the theory that the onset of convection is delayed as the Darcy number is decreased. The effect of Da on the onset of convection and heat transfer is further supported by the experimental data for 3 mm, 6 mm, and 25 mm glass-glycol porous systems presented in Figs. 6a and 6b. Again, a delay in the onset of convection with a decrease in Da is observed. The critical value of Ra_f for the 3 mm glass-glycol porous layer ($Da = 1.53 \times 10^{-6}$) is seen to be $Ra_{f,c} = 5 \times 10^7$, whereas for 6 mm glass-glycol layer ($Da = 9.34 \times 10^{-6}$) $Ra_{f,c} = 1.25 \times 10^7$. Also, similar to what has been observed for the glass-water media (Fig. 4a), the heat transfer curves for the 3 mm and 6 mm glass-glycol media are almost parallel, whereas the slope of the curve for 25 mm glass-glycol porous layer ($Da = 1.85 \times 10^{-4}$) decreases substantially.

Effect of Prandtl Number

The effect of the fluid Prandtl number can be studied by considering the data for porous systems of the same solid material and particle size but of different saturating fluid. Keeping the size of the particle constant eliminates the effect of the Darcy number, to a large extent. On the other hand, a slight variation in the conductivity ratio due to the use of different saturating fluid cannot be avoided (Table 1).

A compilation of the experimental results for 3 mm, 6 mm, and 25 mm glass beads with water and ethylene glycol as saturating fluids (Fig. 7a) clearly shows the trend of increasing heat transfer with increasing Prandtl number at all Darcy and Rayleigh numbers. Indeed, the fluid Nusselt number for glass-glycol porous media ($Pr_f \approx 120$) are higher than the Nu_f for glass-water porous systems ($Pr_f \approx 5.5$) of the same particle size. The effect of Pr_f is seen to increase with an increase in particle size, due to the reduced contribution of Forchheimer's inertial term. Similar effect of Prandtl number is observed in the results for 15.87 mm steel beads (Fig. 7b). It should be noted that the increase in Nusselt number is actually a combined effect of the Prandtl number and the conductivity ratio. For example, the conductivity ratio for glass-water porous systems, $\lambda \approx 0.75$, is lower than that for glass-glycol porous systems, $\lambda \approx 0.45$, which further strengthens the effect of Prandtl number, as also predicted by the numerical solutions. This explains the stronger effect of the fluid Prandtl number in the case of porous layers as compared to fluid layers.

Effect of Conductivity Ratio

The effect of the conductivity ratio, $\lambda = k_f/k_m$, can be studied if we consider the results for porous systems of the same fluid component and similar particle size but of different solid component. In this case, Darcy and fluid Prandtl numbers are almost constant, and the parameter to affect the heat transfer, at a fixed Rayleigh number, is the conductivity ratio. Figure 8a presents the experimental data for 15 mm glass-water ($\lambda = 0.79$), 12.7 mm acrylic-water ($\lambda = 1.75$), and 15.87 mm steel-water ($\lambda = 0.17$) media. The Nusselt number is seen to increase as λ decreases, or the conductivity of the solid particles increases. This is mainly due to an increase in heat transfer by diffusion and dispersion through the solid phase, compared to the convective heat transfer. Similar effect on λ can be observed at higher Pr_f, as shown in Fig. 8b, where the 15.87 mm steel-glycol ($\lambda = 0.142$) Nu_f are higher than the 25 mm glass-glycol ($\lambda = 0.491$) Nu_f, which, in turn, are higher than Nu_f for 25.4 mm acrylic-glycol medium ($\lambda = 1.217$). On the other hand, the effect of conductivity ratio is seen to diminish as Ra_f and/or Da increases. This is demonstrated in Fig. 8c, which is a compilation of the experimental results for 15.87 mm steel-heptane ($\lambda = 0.142$), 25 mm glass-heptane ($\lambda = 0.36$), and 25.4 mm acrylic-heptane ($\lambda = 0.93$). It is easy

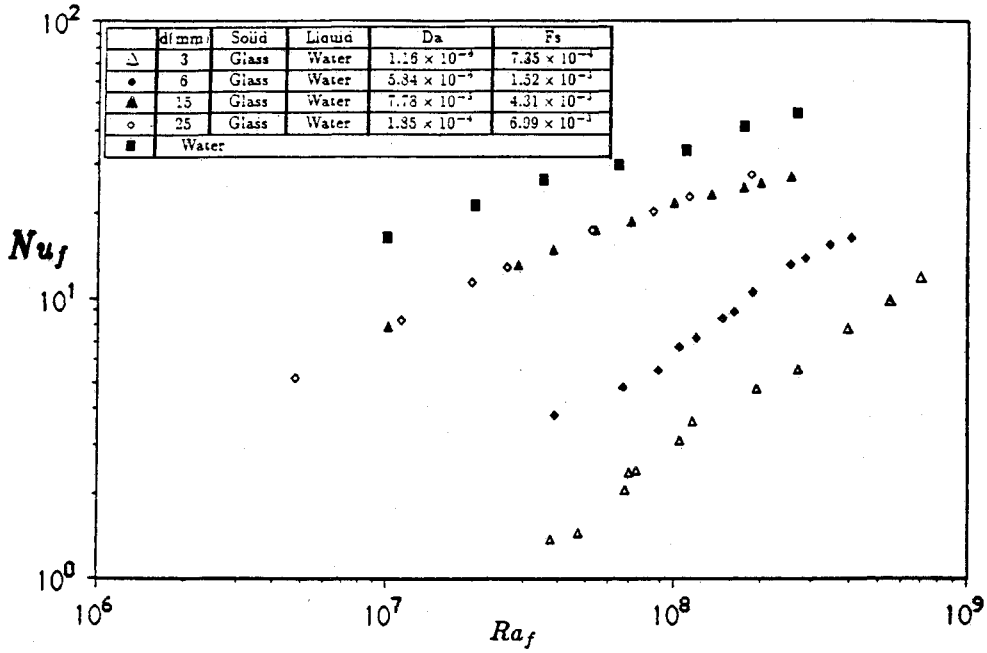

a) Water-glass media and pure water

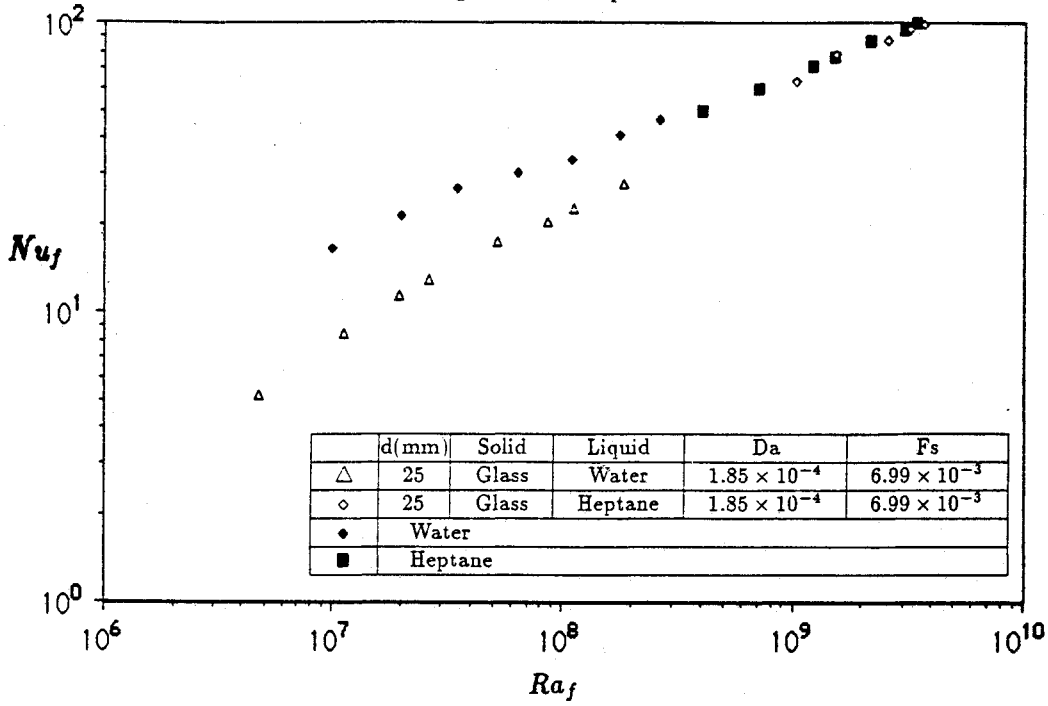

b) Glass-water, glass-heptane, water, and heptane

Fig. 4 Effect of the particle size (Darcy and Forchheimer numbers).

to see that, for $Ra_f > 10^9$, the effect of the conductivity ratio has diminished, and the glass-heptane and acrylic-heptane curves approach each other. On the other hand, although the Darcy number for steel-heptane medium ($Da = 6.84 \times 10^{-5}$) is lower than the Da for glass-heptane ($Da = 1.85 \times 10^{-4}$) and acrylic-heptane ($Da = 1.97 \times 10^{-4}$) media, its effect on Nu_f is negligible, due to the asymptotic behavior clearly demonstrated by the experimental and theoretical results. In this case, the effect of the high-conductivity steel beads (lower λ) is stronger than the effect of Da and, therefore, the steel-heptane Nu_f are slightly higher than the glass-heptane and acrylic-heptane Nu_f. Moreover, when $k_s >> k_f$, the fluid Nusselt number for the porous medium at high Ra_f may be higher than Nu_f for the fluid layer, as shown in Fig. 9, which presents the experimental results for 15.87 mm steel-water, pure water, 15.87 mm steel-heptane, and pure heptane-filled cavity. Indeed, at low Rayleigh numbers, $Ra_f < 10^9$, the heat transfer rates for the porous medium are much lower than the heat transfer rates for the pure liquid layer, but, as Ra_f increases, the Nusselt number curves approach each other.

Comparison With Theoretical Solutions

One of the major goals of the present study was to examine the suitability of the mathematical model based on the DBF equation of motion. This has been done by obtaining numerical solutions[19-22] for a horizontal porous layer of $A = 5$ and the measured values of the governing parameters, and comparing them with the experimental data.

The fact that, for a horizontal layer of $A = 5$, multiple steady-state solutions, which depend on the initial conditions, are possible, introduces a point of ambiguity when a comparison with the experimental data is attempted. Indeed, when

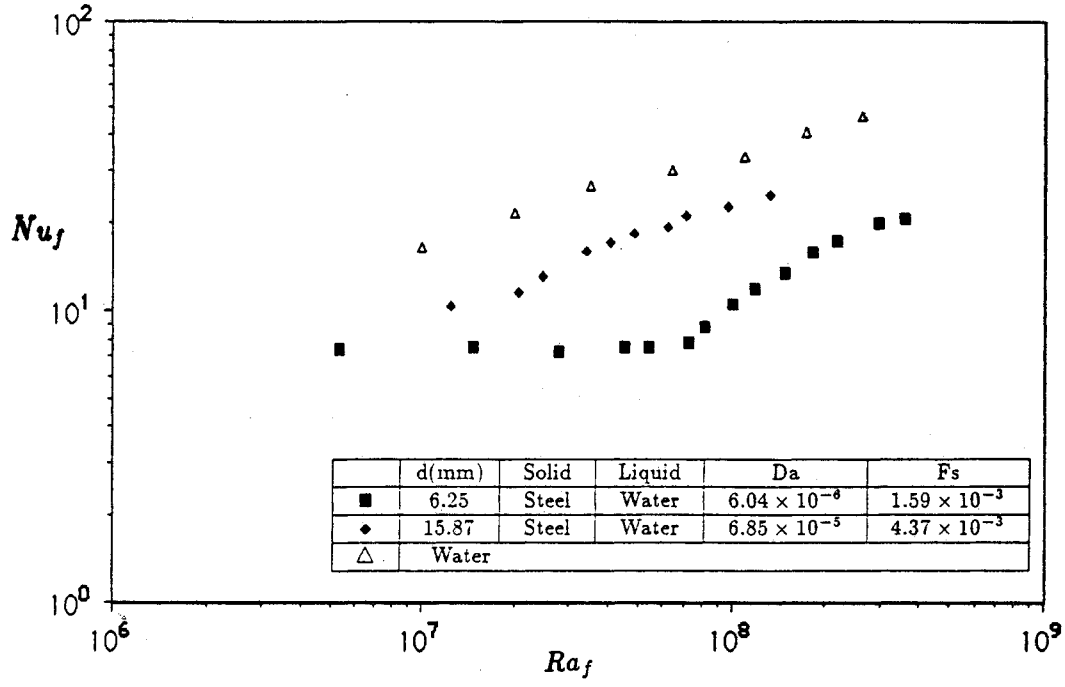

Fig. 5 Nusselt numbers for steel-water and water-filled cavity.

the aspect ratio is larger than unity, either single or multiple cellular convection can take place. The variety of convective patterns obtained in our theoretical study for a cavity of $A = 5$[22] clearly suggests that, for $A > 1$, a more complex bifurcation is obtained, where not only the transitions from conduction to stable convection and from stable convection to oscillatory convection are possible, but where a transition from single to multiple cell convection also can occur. However, the mechanisms for selecting the preferred wavenumber, or the number of convective cells in a cavity of finite horizontal extent, is a difficult task. The validity of the various principles that have been proposed is difficult to assess, especially since different values of the preferred wavenumber are predicted by employing different principles. Since the heat transfer depends on the number of convective rolls,[17] in the multicellular convection regime the number of cells play an important role in the prediction of the energy transport.

In obtaining numerical solutions, an initial condition in the form of sinusoidal waves is generally employed, particularly for the ($m = 1$) convection in a square cavity, $A = 1$.[7,9,19-22] To avoid the ambiguity in the selection of wavenumber m, in the case of $A = 5$, we have decided to use the measured temperature distributions on the bottom and top walls of the cavity. Since it is almost impossible to obtain perfectly isothermal conditions in the laboratory, the small deviations of the temperatures on the bottom and top surfaces from the average values allow initiation of the numerical calculations even if we introduce zero initial conditions in the interior of the cavity. This approach is more realistic, since we do not have to initialize the temperature field in any particular way. It should, however, be noted that it is very difficult to predict how the steady-state temperature distributions on the bottom and top surfaces are affected by the initial power input, since that input has been varied several times in the experiments before the steady-state was reached. Numerical calculations show that, for a particular medium, the Nusselt numbers predicted by employing a sinusoidal temperature distribution as initial condition are, generally, higher than that predicted by following the above approach. However, the difference between any two predictions (one based on sinusoidal perturbation and the other obtained from experimental conditions) corresponding to the same medium and same Ra_f are always less than 13% for the trial runs.[22]

A series of calculations are made to answer the following questions:

1) Is it possible to obtain good agreement with the experimental results by employing the DBF flow model?

2) How important is the flow maldistribution and channeling due to porosity variation in the wall region?

3) How important is the augmentation of the medium thermal conductivity, due to dispersive effects, in improving the agreement between the numerical predictions and the experimental results?

To obtain answers to these questions, the computations have been performed in several stages: DBF solutions with uniform porosity, DBF solutions with variable porosity and variable thermal conductivity in the wall-region, and DBF formulation with dispersive thermal conductivity.

DBF Solutions with Uniform Porosity

Table 2 shows that the DBF solutions compare well with the experimental results only at low Ra_f and Da. At high values of Ra_f and/or Da, these solutions are far from being in reasonable quantitative agreement with the experimental data. On the other hand, the Darcy solution overpredicts the experimental results at high Darcy numbers. For example, the Darcy model yields Nu_f 21.9% higher than the measured Nu_f for 15 mm glass-water porous layer ($Da = 7.78 \times 10^{-5}$, $Ra_f = 2.9 \times 10^7$). Similar disagreement with the DBF solutions (ε constant) has been reported by David et al.[23] Therefore, the next step is to investigate the effects of flow channeling and variable conductivity due to nonuniform porosity in the wall region.

DBF Solutions with Variable Porosity

Here, we shall present the DBF solutions [a modified form of Eqs. (5a-c) with variable porosity in the wall region] according to

$$\varepsilon = \varepsilon_\infty[1 + C_1 \exp(-N_1 X/\gamma)] \qquad (13)$$

where X is the dimensionless distance from the vertical walls. Similar expressions can be written for other walls.[21,22] In accounting for the variation in porosity, we have to select the appropriate values of the empirical constants C_1 and N_1.[29-31] It has been observed that the Ergun model with wall porosity

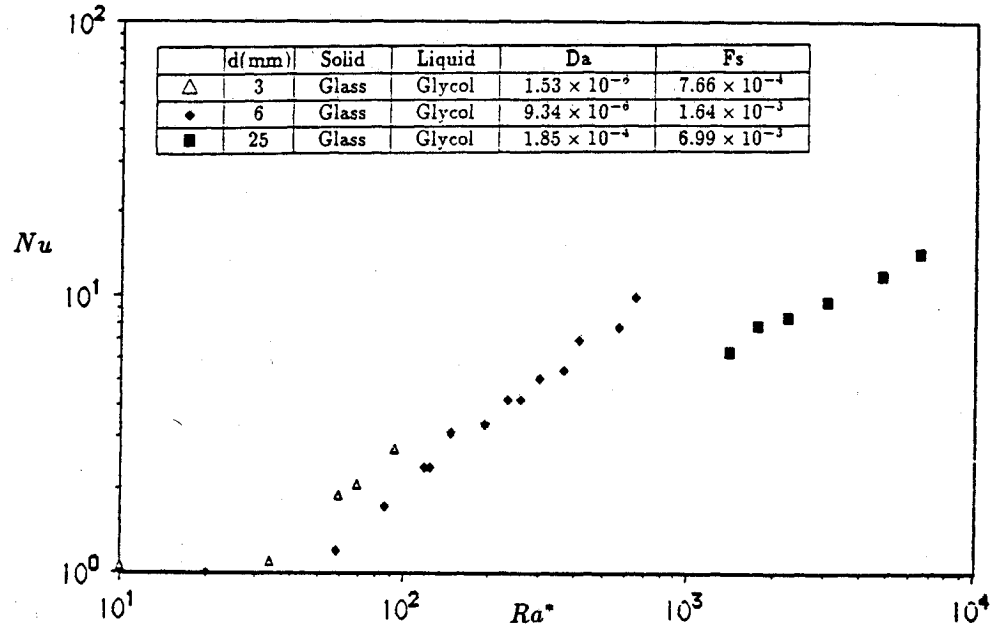

a) Glass-glycol media, Nu vs Ra^*

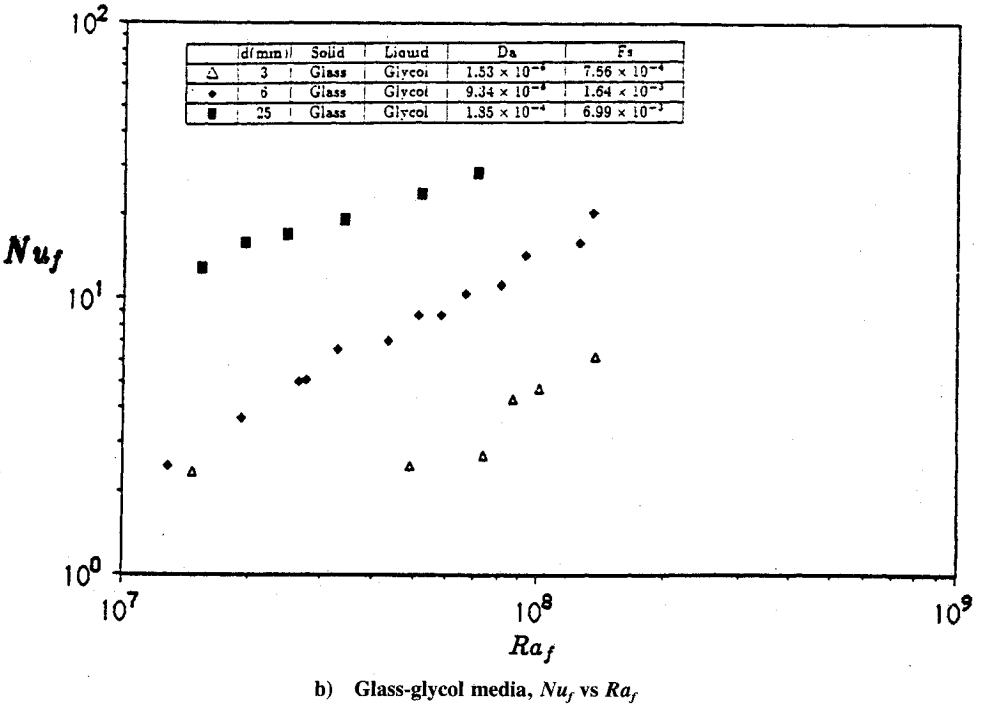

b) Glass-glycol media, Nu_f vs Ra_f

Fig. 6 Effect of Darcy number.

$0.56 \leq \varepsilon_w \leq 0.588$ predicts velocity distributions in the wall region very close to that of the measured ones. On the other hand, as noted by Vafai,[32] the measurements of Price reveal that the flow channeling effects are restricted to wall regions of about two beads diameter thickness. Hence, the present computations have been performed with appropriate values of C_1 and N_1 to achieve $\varepsilon_w = 0.56$ and obtain the asymptotic value of porosity ε_∞ within two beads diameter distance from the wall. It should be emphasized that the above approach is more or less empirical, the exact value of the wall porosity is an issue requiring further investigation. However, initial calculations with $\varepsilon_w \approx 0.86$, as suggested by Vafai,[32] have shown that this choice of ε_w yields numerical solutions that agree well with the measurements for porous media of small particle diameter, but that overpredict the experimental results at high Ra_f and Da. This is clearly demonstrated in Table 3 for the trial cases. The variation in the stagnant thermal conductivity with ε was accounted for as described by the correlation of Krupiczka.[24]

As expected from our numerical study[21,22] and others,[23,27] the inclusion of porosity variation in the DBF model results in higher heat transfer rate predictions. The effect is more pronounced at high Rayleigh numbers and/or Darcy numbers (or large bead diameters). For example, in the case of 3 mm glass-water medium ($Da = 1.16 \times 10^{-6}$), Nu_f increases by 9.6% at $Ra_f = 5.55 \times 10^8$ when the variation in ε is considered (Table 2). When Da increases to 5.84×10^{-6} (6 mm glass-water medium), the percentage change in Nu_f increases to 15.47%, although the Rayleigh number has decreased to 1.48×10^8. The effect is more pronounced in the case of 15 mm glass-water media ($Da = 7.78 \times 10^{-5}$), where the increase in Nu_f is 27.33% at $Ra_f = 1.01 \times 10^7$. The primary reason

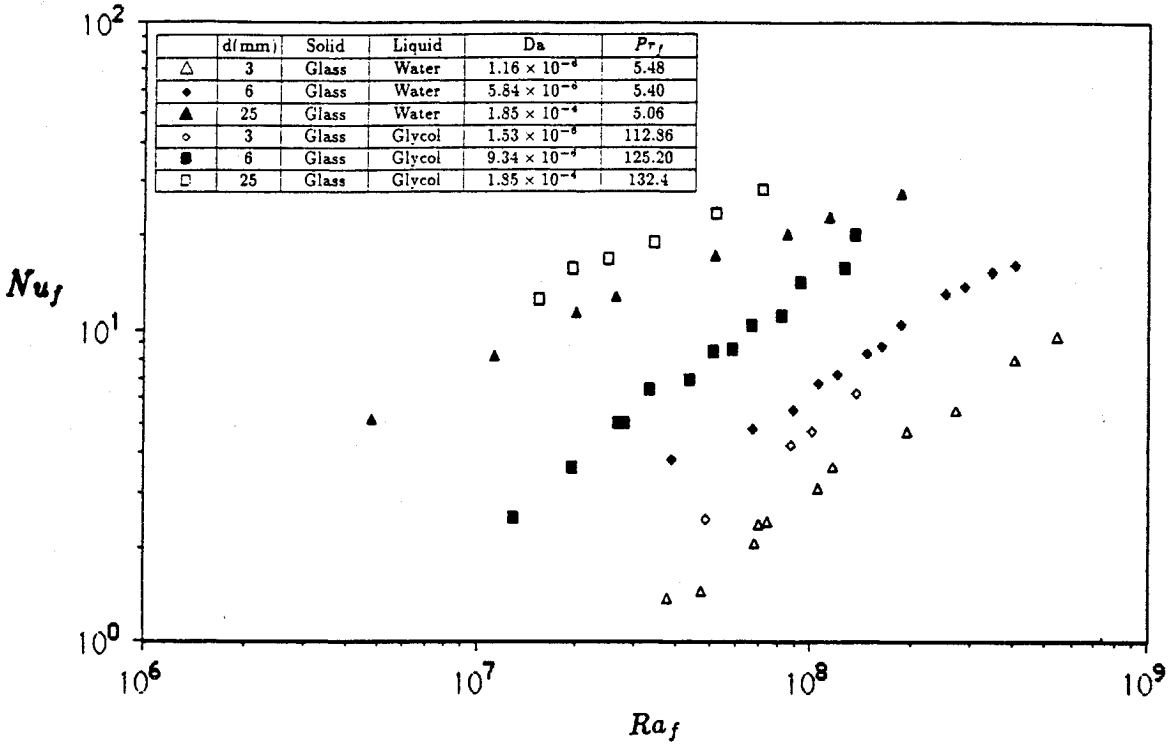

	d(mm)	Solid	Liquid	Da	Pr_f
△	3	Glass	Water	1.16×10^{-6}	5.48
◆	6	Glass	Water	5.84×10^{-6}	5.40
▲	25	Glass	Water	1.85×10^{-4}	5.06
◇	3	Glass	Glycol	1.53×10^{-6}	112.86
■	6	Glass	Glycol	9.34×10^{-6}	125.20
□	25	Glass	Glycol	1.85×10^{-4}	132.4

a) Glass-water and glass-glycol media

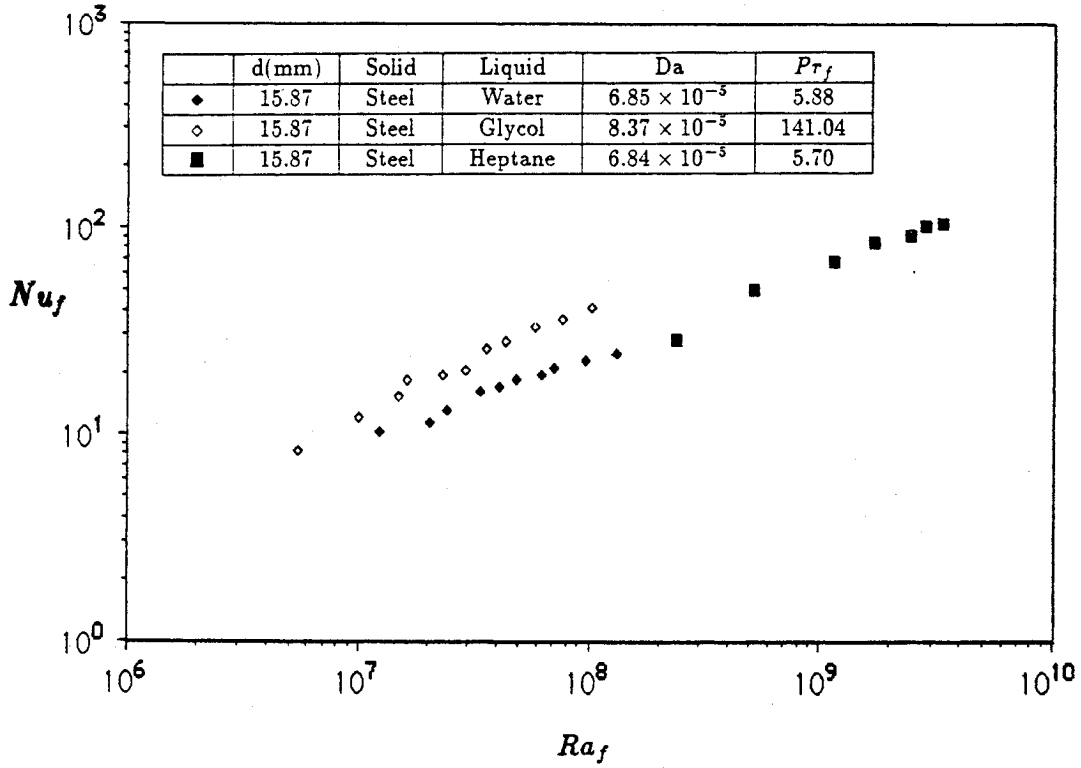

	d(mm)	Solid	Liquid	Da	Pr_f
◆	15.87	Steel	Water	6.85×10^{-5}	5.88
◇	15.87	Steel	Glycol	8.37×10^{-5}	141.04
■	15.87	Steel	Heptane	6.84×10^{-5}	5.70

b) Steel as solid beads and water, heptane and glycol as saturating fluids

Fig. 7 Effect of Prandtl number.

for this enhancement in heat transfer is the increase in convective velocities near the boundaries, which results in strong boundary layers on the horizontal walls.[21–23,27]

The most interesting aspect of our comparison in Table 2 is that the numerical predictions of the DBF formulation with variable porosity are in excellent agreement with the experimental results even at high Rayleigh numbers and large particle sizes. This is true not only for glass-water media but also for acrylic-water and glass-glycol. To further confirm the validity of our conclusions, we have extended our calculations to other experimental sets in a large range of Ra_f, Pr_f, Da, and λ (Table 4). The comparison cannot be extended to all experimental sets, due to the limitations on numerical solutions imposed by the bifurcation to oscillatory flows at high Rayleigh numbers. It should be noted that the oscillatory phenomena were not observed in the experimental work for moderately high values of Ra_f and Da. Due to the stabilizing effect of the heated and cooled plates on the recorded tem-

perature distributions (on the bounding surfaces), we did not observe any appreciable fluctuations in the thermocouple responses.

Table 4 shows that the agreement is excellent for all porous systems, except for steel-water and steel-glycol media, where considerable differences between the numerical predictions and the experimental results are encountered. (This agrees fully with the observation made by David et al.[23]) It should be pointed out that it was not possible to obtain numerical solutions for high-permeability media even at low Ra^*, since both the Fluid Rayleigh and Darcy numbers were very high. For example, Ra_f and Da for $Ra^* = 100$ and $d = 25.4$ mm are 5×10^5 and 2×10^{-4}, respectively.

The present experimental results for porous systems of small particle size ($Da \approx 10^{-6}$) indicate an inflection point in the Nusselt number curves at $Ra^* \approx 300$ (Fig. 2a). The exact value of Ra^* where this transition occurs is a function of the solid-fluid combination and the particle size, but always lies within the range $250 \leq Ra^* \leq 320$. The same trend was observed by Combarnous[5] for small particle size, glass-water porous systems, and has been characterized as the occurrence of a new linearly unstable mode. However, our numerical results for a cavity of $A = 5$ show that the oscillatory convection starts at much higher Ra^* (≈5000). The agreement between our DBF solutions and the experimental results for $Ra^* \geq 300$ gives an alternative explanation. Indeed, the numerical results show that for $Da = 10^{-6}$, the wall channeling effect becomes important for $Ra^* > 300$,[21] and accounts for

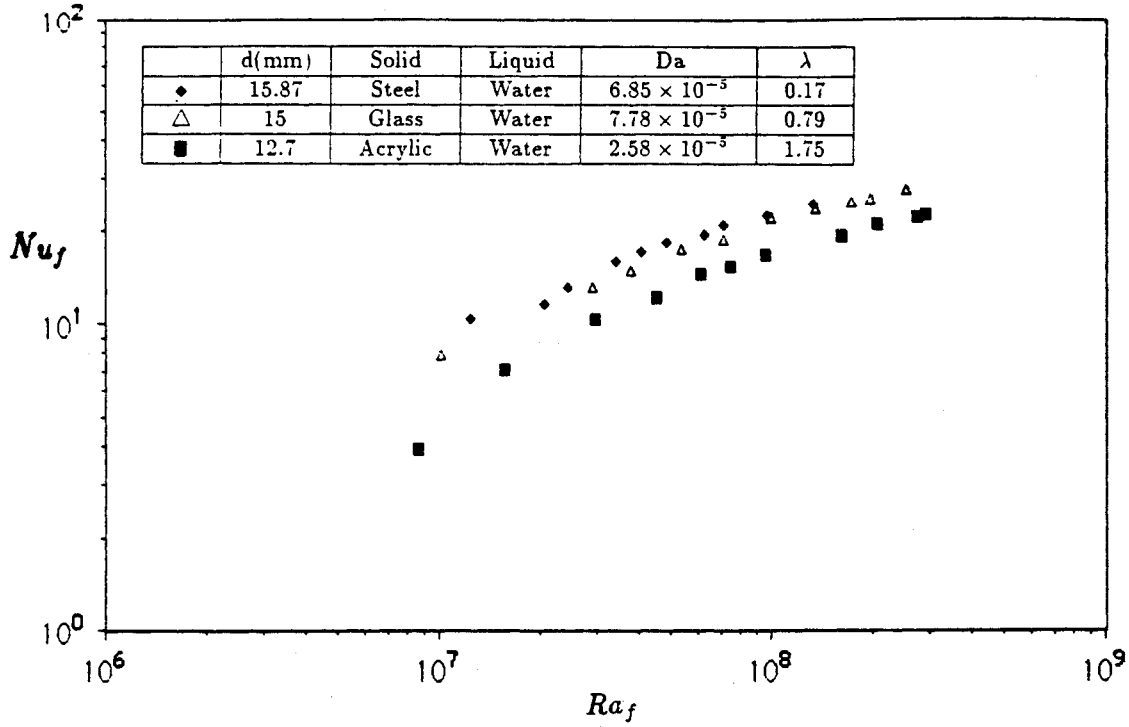

	d(mm)	Solid	Liquid	Da	λ
◆	15.87	Steel	Water	6.85×10^{-5}	0.17
△	15	Glass	Water	7.78×10^{-5}	0.79
■	12.7	Acrylic	Water	2.58×10^{-5}	1.75

a) Steel-water, glass-water, and acrylic-water media

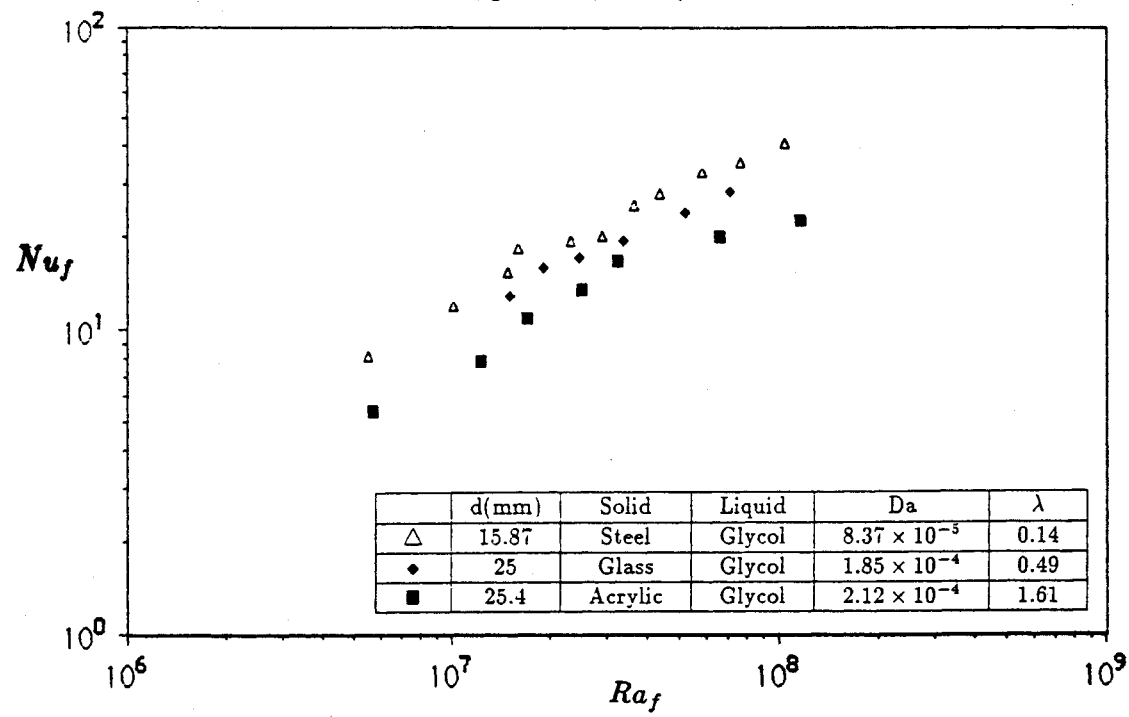

	d(mm)	Solid	Liquid	Da	λ
△	15.87	Steel	Glycol	8.37×10^{-5}	0.14
◆	25	Glass	Glycol	1.85×10^{-4}	0.49
■	25.4	Acrylic	Glycol	2.12×10^{-4}	1.61

b) Steel-glycol, glass-glycol, and acrylic-glycol media

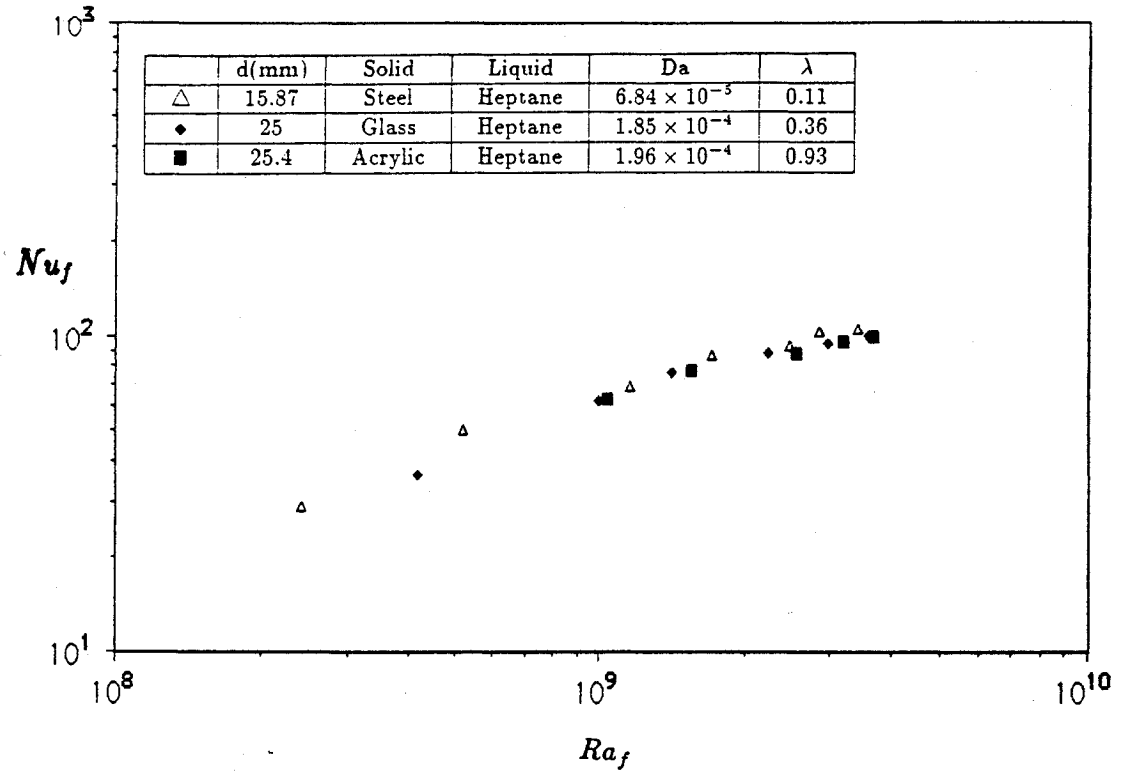

c) Steel-heptane, glass-heptane, and acrylic-heptane media

Fig. 8 Effect of thermal conductivity ratio.

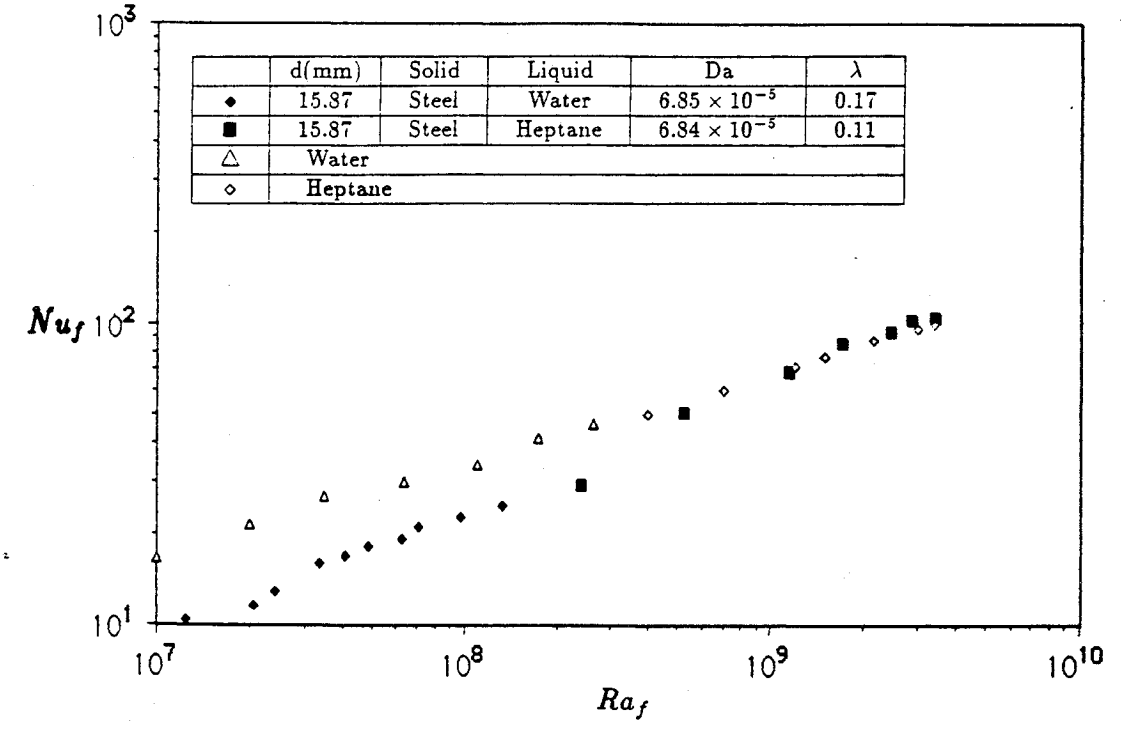

Fig. 9 Comparison between water and heptane data with that of steel-water and steel-heptane media.

the change in the slope of the *Nu* vs *Ra** curve due to the enhancement in the heat transfer rates. This, however, needs to be investigated further.

DBF Solutions with Dispersive Conductivity

In considering the augmentation of thermal conductivity due to dispersive effects, the effective conductivity, according to the stochastic phenomenological model developed by Georgiadis and Catton,[18] for isotropic porous media, has been employed:

$$k^* = k_m + Di|\underline{V}|I \tag{14}$$

where Di is the dispersion factor, defined as

$$Di = D[k_f/(1 - \varepsilon)](d/H) \tag{15}$$

Table 2 Comparison between measured and predicted values of Nusselt number-DBF formulation with and without consideration of variable porosity

Set no.	Fluid-solid	d, mm	$Da \times 10^6$	Pr_f	λ	$Ra_f \times 10^{-7}$	Nu_f exp.	Nu_f DBF	Nu_f DBF+ var. ε, λ
1	WG[a]	3	1.16	5.5	0.73	55.5	8.78	7.29	7.99
2	WG	6	5.84	5.4	0.74	3.85	3.82	3.33	3.62
						14.8	8.48	7.24	8.76
3	WG	15	77.8	5.1	0.79	1.01	7.84	6.07	7.73
						2.89	13.10	11.05	13.27
5	WA	12.7	25.8	5.7	1.75	0.87	3.93	3.32	3.86
						2.90	10.06	7.74	9.53
10	GlG	6	9.34	125.2	0.48	9.25	14.24	11.77	13.81
						12.5	15.91	12.68	15.72

[a]W-water, Gl-Glycol, G-Glass, A-Acrylic, and S-Steel.

Table 3 Comparison between measured and predicted values of Nusselt number-DBF formulation with consideration of variable porosity $_w \approx 0.86$ and $_w \approx 0.56$

Set no.	Fluid-solid	d, mm	$Da \times 10^6$	Pr_f	λ	$Ra_f \times 10^{-7}$	Nu_f exp.	Nu_f $\varepsilon_w \approx 0.86$	Nu_f $\varepsilon_w \approx 0.56$
1	WG	3	1.16	5.5	0.73	55.5	8.78	8.22	7.99
2	WG	6	5.84	5.4	0.74	14.8	8.48	9.35	8.76
3	WG	15	77.8	5.1	0.79	1.01	7.84	9.45	7.73
5	WA	12.7	25.8	5.7	1.75	0.87	3.93	4.35	3.86
7	WS	6.35	6.04	5.6	0.13	29.6	20.22	29.15	24.85
10	GlG	6	9.34	125.2	0.48	8.09	11.23	11.69	10.74

Table 4 Comparison between measured and predicted values of Nusselt number-DBF formulation with variable porosity and variable thermal conductivity in the wall regions

Set no.	Fluid-solid	d, mm	$Da \times 10^6$	Pr_f	λ	$Ra_f \times 10^{-7}$	Nu_f exp.	Nu_f DBF+ var.ε, λ
1	WG	3	1.16	5.48	0.73	6.80	2.06	2.14
						19.4	4.70	4.79
						27.1	5.55	5.65
						55.5	8.78	7.99
						73.2	11.58	10.47
2	WG	6	5.84	5.40	0.79	3.85	3.82	3.62
						6.70	5.54	6.08
						14.8	8.48	8.76
						25.2	13.14	13.52
3	WG	15	77.8	5.06	0.79	1.01	7.84	7.73
						2.89	13.10	13.27
5	WA	12.7	25.8	6.21	1.75	0.87	3.93	3.86
						1.54	6.90	6.37
						2.90	10.06	9.53
7	WS	6.35	6.04	5.64	0.13	18.2	16.34	18.92
						29.6	20.22	24.85
						35.9	21.45	26.38
9	GlG	3	1.53	112.86	0.44	13.7	6.22	6.96
10	GlG	6	9.34	125.20	0.48	2.64	5.03	6.10
						3.29	6.54	6.44
						5.13	8.65	8.70
						8.09	11.23	10.74
						9.25	14.24	13.81
						12.5	15.91	15.72
13	GlG	15.87	83.7	141.04	0.14	1.01	11.98	20.52
						1.50	15.41	25.72
						3.63	25.62	38.80
						4.35	27.68	44.20

In principle, the value of the dispersion coefficient D in Eq. (16) depends on the type of packing of the bed. We have performed calculations with $D = 0.36$, which value has been shown by Georgiadis and Catton to provide the best fit of the measurements for k^*.

The quantitative results of our study are presented in Table 5. For comparison purposes, the experimental Nu_f and the Nusselt number predicted by the DBF formulation with and without variable porosity are also listed in Table 5. It is seen that, for the range of Rayleigh numbers considered here,

Table 5 Effect of dispersive conductivity on numerical predictions

Set no.	Fluid-solid	d, mm	Ra_f	Nu_f exp.	Nu_f DBF	Nu_f DBF + var. ε, λ	Nu_f DBF + disp
1	WG	3	5.55×10^8	8.78	7.29	7.99	8.52
7	WS	6.35	1.82×10^8	16.34	17.40	18.92	21.38
			3.59×10^8	21.45	24.01	26.38	32.15
13	GlS	15.87	1.50×10^7	15.41	21.60	26.72	25.93
			3.63×10^7	25.62	33.12	38.80	41.08
			4.35×10^7	27.68	36.96	44.20	46.94

dispersion effects always increase the heat transfer coefficient. The increase in Nu_f depends on the particle diameter. For small particle size (3 mm glass-water), the difference between the Nusselt number predicted by the DBF formulation and that predicted by the DBF formulation with dispersive conductivity [Eq. (14)] is about 17% ($Ra_f = 5.55 \times 10^8$). As d increases, the velocity and temperature gradients decrease, but the dispersive conductivity increases proportionally to γ [Eq. (14)]. The net effect on the difference between the Nusselt numbers predicted by the two formulations is that the difference reaches a maximum value and then decreases. This is obvious from Table 5: the difference in Nu_f for 6.35 mm steel-water medium ($Ra_f = 3.59 \times 10^8$) is 34%, but for 15.87 mm steel-glycol medium the difference in Nu_f is 27%. The above trend is in agreement with the results of Georgiadis and Catton.[18]

Nevertheless, all the numerical predictions by the DBF formulation with the augmentation of the thermal conductivity due to dispersive effects here being considered are higher than the values predicted by the DBF formulations, and much higher than the experimental results in the case of steel-water and steel-glycol porous systems. Also, similar to what has been observed for the DBF model, the DBF formulation with the dispersive conductivity is expected to yield even higher predictions, when the variation in porosity in the wall region is considered. The inclusion of dispersive effects do not seem to provide an answer for the discrepancy between the predictions and the experimental data for porous systems involving steel beads as the solid matrix.

Conclusions

The experimental results for horizontal porous layers of $A = 5$ fully support the effects of the governing parameters, as predicted by the theoretical solutions based on the DBF flow model. The heat transfer rate is seen to increase with Darcy number (or particle size), Rayleigh number, and Prandtl number, and decrease as the conductivity ratio increases. The experimental data for porous systems of the same solid-fluid combination, but different particle size, indicate the existence of an asymptotic convection regime ($d > 15$ mm), where the heat transfer rates are almost independent of the particle size (or the Darcy number), as also predicted by the DBF solutions. The effect of the conductivity ratio is seen to be more pronounced at low Rayleigh and/or Darcy numbers, and diminishes as Ra_f and Da increase. Moreover, by employing the DBF formulation with variable porosity, we have succeeded in achieving an excellent agreement between the experimental results and numerical predictions, even at high Rayleigh numbers and large particle sizes, which are two of the conditions under which the Darcy solutions always fail to agree with the measurements.

Good agreement between numerical and experimental results have been obtained, also, for systems with $k_s \approx k_f$, such as acrylic-water and glass-glycol. On the other hand, it has not been possible to achieve a reasonable agreement in the case of a highly conducting porous matrix (steel beads). The strong conduction through the solid particles seems to stabilize the flow and reduce the Nusselt number much more than predicted by the DBF formulations. No improvement has been realized by considering the dispersive effects through a first-order relation between the dispersive conductivity and the filtration velocity. A more refined solution could possibly be obtained by treating the medium as a fluid-solid heterogeneous system and using separate energy transport equations for the two phases.

Acknowledgments

The authors gratefully acknowledge the support of this work by the National Science Foundation, Grant No. 85-04100.

References

[1]Combarnous, M., and Bories, S., "Hydrothermal Convection in Saturated Porous Media," *Advances in Hydroscience*, Vol. 1, 1975, pp. 231–307.

[2]Cheng, P., "Heat Transfer in Geothermal Systems," *Advances in Heat Transfer*, Vol. 14, 1978, pp. 1–105.

[3]Catton, I., "Natural Convection in Porous Media," *Natural Convection Fundamentals and Applications*, edited by S. Kakac et al., Hemisphere, NY, 1985, pp. 514–547.

[4]Schneider, K. J., "Investigation of the Influence of Free Thermal Convection on Heat Transfer Through Granular Material," *Proceedings of International Inst. of Refrigeration*, Vol. II–4, 1963, pp. 247–253.

[5]Combarnous, M., "Convection Naturelle et Convection Mixte Dans une Couche Poreuse Horizontale," *Revue Generale de Therminique*, Vol. 108, 1970, pp. 1350–1376.

[6]Buretta, R. J., and Berman, A. S., "Convective Heat Transfer in a Liquid Saturated Porous Layer," *Journal of Applied Mechanics*, Vol. 43, June 1976, pp. 249–253.

[7]Caltagirone, J. P., "Thermoconvective Instabilities in a Horizontal Porous Layer," *Journal of Fluid Mechanics*, Vol. 72, Part 2, 1975, pp. 269–287.

[8]Schubert, G., and Straus, J. M., "Three-dimensional and Multicellular Steady and Unsteady Convection in Fluid-saturated Porous Media at High Rayleigh Numbers," *Journal of Fluid Mechanics*, Vol. 94, 1979, pp. 25–38.

[9]Kimura, S., Schubert, G., and Straus, J. M., "Route to Chaos in Porous Medium Thermal Convection," *Journal of Fluid Mechanics*, Vol. 166, 1986, pp. 305–324.

[10]Jonsson, T., and Catton, I., "Prandtl Number Dependence of Natural Convection in Porous Media," *Journal of Heat Transfer*, Vol. 109, No. 2, 1987, pp. 371–377.

[11]Seki, N., Fukusako, S., and Inaba, H., "Heat Transfer in a Confined Rectangular Cavity Packed with Porous Media," *International Journal of Heat and Mass Transfer*, Vol. 21, No. 7, 1978, pp. 985–989.

[12]Somerton, C. W., "The Prandtl Number Effect in Porous Layer Convection," *Applied Sciences Research*, Vol. 40, No. 4, 1983, pp. 333–344.

[13]Prasad, V., Kulacki, F. A., and Keyhani, M., "Natural Convection in Porous Media," *Journal of Fluid Mechanics*, Vol. 150, 1985, pp. 89–119.

[14]Wang, M., and Bejan, A., "Heat Transfer Correlation for Benard Convection in a Fluid Saturated Porous Layer," *International Communications in Heat and Mass Transfer*, Vol. 14, 1987, pp. 617–626.

[15]Rudraiah, N., "Non-linear Convection in a Porous Medium with Convective Acceleration and Viscous Force," *Arabian Journal of Science and Engineering*, Vol. 9, No. 2, 1984, pp. 153–167.

[16]Kvernvold, O., and Tyvand, P. A., "Nonlinear Thermal Convection in Anisotropic Porous Media," *Journal of Fluid Mechanics*, Vol. 90, Part 4, 1979, pp. 608–624.

[17]Georgiadis, J. G., and Catton, I., "Prandtl Number Effect on Benard Convection in Porous Media," *Journal of Heat Transfer*, Vol. 108, No. 2, 1986, pp. 284–290.

[18]Georgiadis, J. G., and Catton, I., "Dispersion in Cellular Ther-

mal Convection in Porous Layers," *International Journal of Heat and Mass Transfer*, Vol. 31, No. 5, 1988, pp. 1081–1091.

[19]Kladias, N., and Prasad, V., "Natural Convection in Horizontal Porous Layers: Effects of Darcy and Prandtl Numbers," *Journal of Heat Transfer*, Vol. 111, No. 4, 1989, pp. 926–935.

[20]Kladias, N., and Prasad, V., "Flow Transitions in Bouyancy-induced Non-Darcy Convection in a Porous Medium Heated from Below," *Journal of Heat Transfer*, Vol. 112, No. 3, 1990, pp. 675–684.

[21]Kladias, N., and Prasad, V., "Convective Instabilities in Horizontal Porous Layers Heated from Below: Effects of Grain size and Its Properties," ASME HTD-Vol. 107, 1989, pp. 369–379, American Society of Mechanical Engineers, New York.

[22]Kladias, N., "Non-Darcy Free Convection in Horizontal Porous Layers," Ph.D. Dissertation, Columbia Univ., New York, NY, 1988.

[23]David, E., Lauriat, G., and Prasad, V., "Non-Darcy Natural Convection in Packed-sphere Beds Between Concentric Vertical Cylinders," *Heat Transfer-Philadelphia, 1989*, AIChE Symposium Series, edited by S. B. Yilmaz, Vol. 85, 1989, pp. 90–95, American Institute of Chemical Engineers, New York.

[24]Prasad, V., Kladias, N., Bandyopadhaya, A., and Tian, Q., "Evaluation of Correlations for Stagnant Thermal Conductivity of Liquid-saturated Porous Beds of Spheres," *International Journal of Heat and Mass Transfer*, Vol. 32, No. 5, 1989, pp. 793–1796.

[25]Beckermann, C., Viskanta, R., and Ramadhyani, S., "A Numerical Study of Non-Darcian Natural Convection in a Vertical Enclosure Filled with a Porous Medium," *Numerical Heat Transfer*, Vol. 10, No. 6, 1986, pp. 557–570.

[26]Lauriat, G., and Prasad, V., "Non-Darcian Effects on Natural Convection in a Vertical Enclosure," *International Journal of Heat and Mass Transfer*, Vol. 32, No. 11, 1989, pp. 2135–2148.

[27]David, E., Lauriat, G., and Cheng, P., "Natural Convection in Rectangular Cavities with Variable Porosity Media," ASME HTD-Vol. 96, 1988, pp. 605–612, American Society of Mechanical Engineers, New York.

[28]Yen, Y. C., "Effects of Density Inversion on Free Convection Heat Transfer in a Porous Layer Heated from Below," *International Journal of Heat and Mass Transfer*, Vol. 17, No. 11, 1974, pp. 1349–1356.

[29]Roblee, L. H., Baird, R. M., and Tierney, J. W., "Radial Porosity Variation in Packed Beds," *AIChE Journal*, Vol. 4, No. 4, 1958, pp. 450–464.

[30]Benenati, R. F., and Brosilow, C. B., "Void Fraction Distribution in Packed Beds," *AIChE Journal*, Vol. 8, No. 3, 1962, pp. 359–361.

[31]Chandrashekara, B. C., and Vortmeyer, D., "Flow Model for Velocity Distribution in Fixed Porous Beds Under Isothermal Conditions," *Warme-und-Stoffubertragung*, Vol. 12, No. 2, 1979, pp. 105–111.

[32]Vafai, K., "Convective Flow and Heat Transfer in Variable-porosity Media," *Journal of Fluid Mechanics*, Vol. 147, 1984, pp. 233–259.